Biosensors and Bioelectronics 162 (2020) 112259

Contents lists available at ScienceDirect

Biosensors and Bioelectronics

journal homepage: http://www.elsevier.com/locate/bios

A 96-well high-throughput, rapid-screening platform of extracellular electron transfer in microbial fuel cells

Mehdi Tahernia [a], Maedeh Mohammadifar [a], Yang Gao [a], Warunya Panmanee [b], Daniel J. Hassett [b], Seokheun Choi [a,*]

[a] Bioelectronics & Microsystems Laboratory, Department of Electrical & Computer Engineering, State University of New York-Binghamton, Binghamton, NY, 13902-6000, USA

[b] Department of Molecular Genetics, Biochemistry& Microbiology, University of Cincinnati College of Medicine, Cincinnati, OH, 45267-0524, USA

ARTICLE INFO

Keywords:
Extracellular electron transfer (EET)
Electrogen
Pseudomonas aeruginosa
Genetic engineering
Microbial fuel cell
High-throughput sensing

ABSTRACT

Microbial extracellular electron transfer (EET) stimulates a plethora of intellectual concepts leading to potential applications that offer environmentally sustainable advances in the fields of biofuels, wastewater treatment, bioremediation, desalination, and biosensing. Despite its vast potential and remarkable research efforts to date, bacterial electrogenicity is arguably the most underdeveloped technology used to confront the aforementioned challenges. Severe limitations are placed in the intrinsic energy and electron transfer processes of naturally occurring microorganisms. Significant boosts in this technology can be achieved with the growth of synthetic biology tools that manipulate microbial electron transfer pathways and improve their electrogenic potential. In particular, electrogenic *Pseudomonas aeruginosa* has been studied with the utility of its complete genome being sequenced coupled with well-established techniques for genetic manipulation. To optimize power density production, a high-throughput, rapid and highly sensitive test array for measuring the electrogenicity of hundreds of genetically engineered *P. aeruginosa* mutants is needed. This task is not trivial, as the accurate and parallel quantitative measurements of bacterial electrogenicity require long measurement times (~tens of days), continuous introduction of organic fuels (~tends of milliliters), architecturally complex and often inefficient devices, and labor-intensive operation. The overall objective of this work was to enable rapid (<30 min), sensitive (>100-fold improvement), and high-throughput (>96 wells) characterization of bacterial electrogenicity from a single 5 μL culture suspension. This project used paper as a substratum that inherently produces favorable conditions for easy, rapid, and sensitive control of an electrogenic microbial suspension. From 95 isogenic *P. aeruginosa* mutant, an *hmgA* mutant generated the highest power density (39 μW/cm^2), which is higher than that of wild-type *P. aeruginosa* and even the strongly electrogenic organism, *Shewanella oneidensis* (25 μW/cm^2). In summary, this work will serve as a springboard for the development of novel paradigms for genetic networks that will help develop mutations or over-expression and synthetic biology constructs to identify genes in *P. aeruginosa* and other organisms that enhance electrogenic performance in microbial fuel cells (MFCs).

1. Introduction

Extracellular electron transfer (EET) is a remarkable bioelectrochemical process utilized by certain microorganisms for growth, overall cell maintenance, and information exchange with surrounding microorganisms or environments (Kumara et al., 2017; Lovley, 2012; Yates et al., 2016). Some of those microorganisms respire even in oxygen-limited environments and produce energy for vital processes by transferring electrons from their intracellular milieu to external insoluble electron acceptors (Slate et al., 2019). Emerging bioelectrochemical technologies, including microbial fuel cells (MFCs), microbial electrolysis cells (MECs), microbial desalination cells (MDCs) and microbial electrosynthesis (MES), are based upon interactions between the microorganisms and the insoluble electron acceptors during reduced oxygen tension or anaerobic conditions (Logan et al., 2019). Some other microbial communities are electrically connected and perform metabolic cooperation via direct interspecies electron transfer (DIET) (Lovley, 2017). DIET allows electrical connections between

* Corresponding author.
E-mail address: sechoi@binghamton.edu (S. Choi).

https://doi.org/10.1016/j.bios.2020.112259
Received 16 January 2020; Received in revised form 22 April 2020; Accepted 28 April 2020
Available online 8 May 2020

electron-donating and electron-accepting microorganisms to share available energy under different environmental conditions. The DIET between interdependent microorganisms makes them highly versatile for various applications including new material synthesis, and anaerobic digestion (Park et al., 2018; Kouzuma et al., 2015). Alternatively, many microbial pathogens such as *Pseudomonas aeruginosa* use quorum sensing inter-cellular communication by producing diffusible signaling molecules (e.g., autoinducers) and redox active compounds to control virulence during infections and defend their immediate niche against competing microorganisms and environmental stresses (Koch and Harnisch, 2016a). The redox-active compounds can also serve as extracellular soluble mediators for microbial EET. Regardless of whether microbial EET is a major mode of microbial metabolism for energy generation or a minor mode for communication, revolutionizing our current knowledge about and application of microbial electrogenic capacity fosters an enormous potential for renewable energy technologies and environmentally sustainable advances.

Various environments, even those involving harsh conditions, are known to host microorganisms performing EET (also named as exoelectrogens, electroactive microorganisms, and electrogens) (Chabert et al., 2015). Recent studies have demonstrated electrogenicity by even Gram-positive microorganisms, which have thick cell walls that limit effective electron transfer (Light et al., 2018). Other microorganisms have been explored to demonstrate weak electrogenic capacity in microbial consortia, involving DIET and EET-involved cell-to-cell communications (Koch and Harnisch, 2016b; E Doyle and Marsili, 2018). However, to date, only about 100 microbial species have been designated as exoelectrogens since microbial EET was first discovered, which is a very short list for a technology that has a history of ~100 years (Koch and Harnisch, 2016b; Schröder, 2011). Moreover, the development of new mutants by genetically engineering microbial metabolic pathways for efficient EET lags behind despite significant technological advances in synthetic biology that strive to manipulate critical electrogenic pathways (TerAvest and Ajo-Franklin, 2016; Alfonta, 2010). This is mainly because conventional measurement techniques to evaluate microbial electrogenicity are based on large-scale MFCs that require a long testing time (several days to months), energy-intensive fluidic feeding systems with large sample volumes, and cumbersome experimental operations (Biffinger et al., 2009; Cao et al., 2009; Hou et al., 2009). Therefore, simultaneous evaluation of multiple microbial samples has been even more challenging while comparison between sporadic experimental results generated by individual researchers with different environmental conditions, device architecture, and materials cannot be properly assessed. In addition, experimental results generated from the large-scale MFC's may not be repeatable or reliable because maintaining the identical environmental condition for the mL-scale or L-scale macro-sized experimental set-up and forming the same composition of electrogenic biofilms are formidably challenging.

Rapidly evolving microfluidics and microelectromechanical systems (MEMS) technologies enabled a few research groups to create high-throughput screening devices with large upside potential (Hou et al., 2009, 2012). However, micro-liter sized sensing units in an array format harbored considerably smaller bacterial titers, decreased electricity generation and the consequent sensitivity of the array for bacterial electrogenic screening. Although microscale devices require a significantly shorter start-up time for microbial biofilm accumulation and acclimation on the electrode than mL-sized macro-MFCs, micro-devices still required ~ tens of hours of start-up time (Qian et al., 2009). Moreover, those microfluidic devices required complex device structures with many fluidic channels and external tubing that require operation using external pumps, ultimately limiting the number of sensing units on the array to at most 24 (Hou et al., 2012).

Other microscale techniques that "*indirectly*" measure microbial EET have also been proposed. Zhou et al. demonstrated a high-throughput electrochrome-based colorimetric method by measuring the peroxidase activity of the multi-heme *c*-type cytochromes, the key components of direct EET in some electrogens (Zhou et al., 2015). Twelve bacterial EET capacities were evaluated on a plate-based colorimetric assay, which was rapid, easily manipulable, and inexpensive. Very recently, Wang et al. created a new technique to indirectly characterize microbial EET by measuring cell polarizability in a microfluidic system (Wang et al., 2019). They showed a strong correlation between microbial EET through *c*-type cytochromes and cell surface polarizability, providing a rapid screening technique even for metabolically fastidious microorganisms. However, both techniques are limited to microorganisms having direct EET mechanisms through *c*-type cytochromes, impeding the investigation of other microorganisms with indirect EET. Furthermore, colorimetric methods normally suffer from low-sensitivity for quantitative measurements, while cell polarizability cannot characterize microbial EET in microbial consortia or in biofilms. Therefore, "*direct*" measurement of microbial electrons transferred from the cell interior is the most accurate and reliable technique to characterize all microbial electrogenic capabilities.

In this work, we created a unique experimental platform to achieve rapid (~30 min), highly sensitive (~75 μA/cm^2) electricity generation from the weak yet genetically tractable exoelectrogen, *P. aeruginosa* PAO1 in each sensing well, which is 100 times higher than the previous MFC array (Mukherjee et al., 2013). We used a high-throughput (96-well) platform to characterize microbial EET in a defined, sub-microliter culture volume (~5 μL) by directly measuring microbial electricity generation in a novel MFC device configuration (Fig. 1). This led to higher throughput, quicker screening and smaller samples than are possible with the 64-well array even with its advantages over existing methods (Tahernia et al., 2019). Microbial electrogenicities of 95 isogenic mutants of *P. aeruginosa* were comprehensively analyzed by simultaneously measuring their polarization curve and output power as a function of current and comparing their maximum power and current density. We used paper as the MFC substratum that inherently produces favorable conditions for easy and rapid control of a sub-microliter microbial sample through the capillary-driven flow without tubes and fluidic feeding systems (Gao et al., 2019; Gao and Choi, 2018). A conductive redox polymer conformally and tightly coated on paper fibers increased the current generation from the 3-D porous electrode surface on which the bacteria are attached. This facilitated microbial EET, resulting in a significant increase in sensitivity. The porous, conductive paper structure ensured a large surface area and efficient mass transfer to and from the paper while the biocompatible redox polymer led to rapid and dense bacterial adhesion as biofilms (Gao et al., 2019). The high-throughput MFCs were batch-fabricated into an array by printing and microfluidic injection processes to build the sensing units on paper. The paper-based sensing array required only simple, reproducible, energy-conserving and inexpensive fabrication processes for large-scale applications. Taken together, this work will accelerate the discovery of new exoelectrogens in various complex environments and drive the development of novel paradigms for genetic networks that will help develop synthetic biology, mutagenic or over-expression constructs and identify which genes in exoelectrogens trigger a higher electrogenic performance.

2. Results and discussion

2.1. A 96-well MFC array design

High-throughput measurement of microbial EET was performed by defining 96 spatially distinct individual reservoirs on Whatman 3 MM chromatographic paper (Fig. 2). A commercially-available wax printer rapidly and accurately printed wax circular patterns on one side of the paper, which were further penetrated vertically to the opposite side upon heat treatment, defining a completely closed hydrophilic reservoirs within (Fig. S1). The dimensions of the reservoir and the array were precisely designed to be compatible with an industry standard 96-well micropipettor by controlling the vertical and horizontal penetration

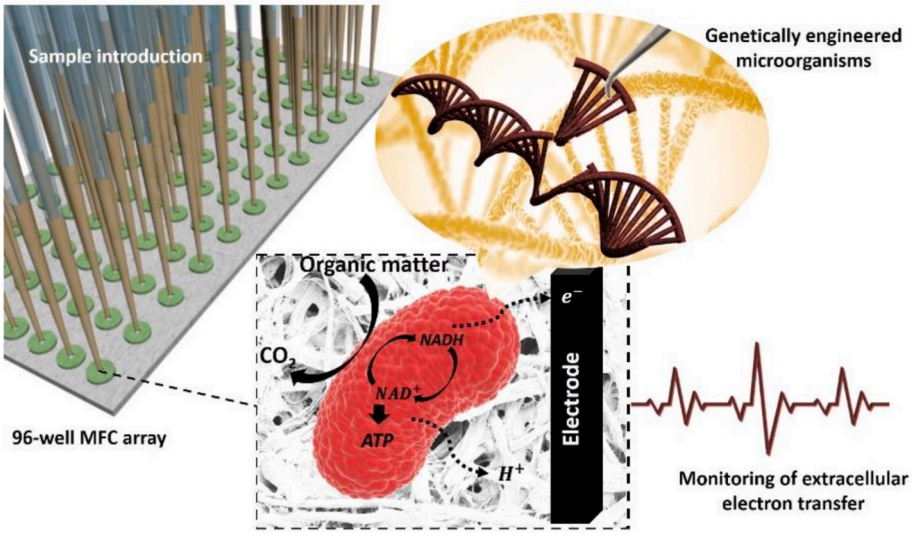

Fig. 1. A conceptual illustration of our high-throughput sensing array for characterization of extracellular electron transfer of genetically engineered *Pseudomonas aeruginosa*.

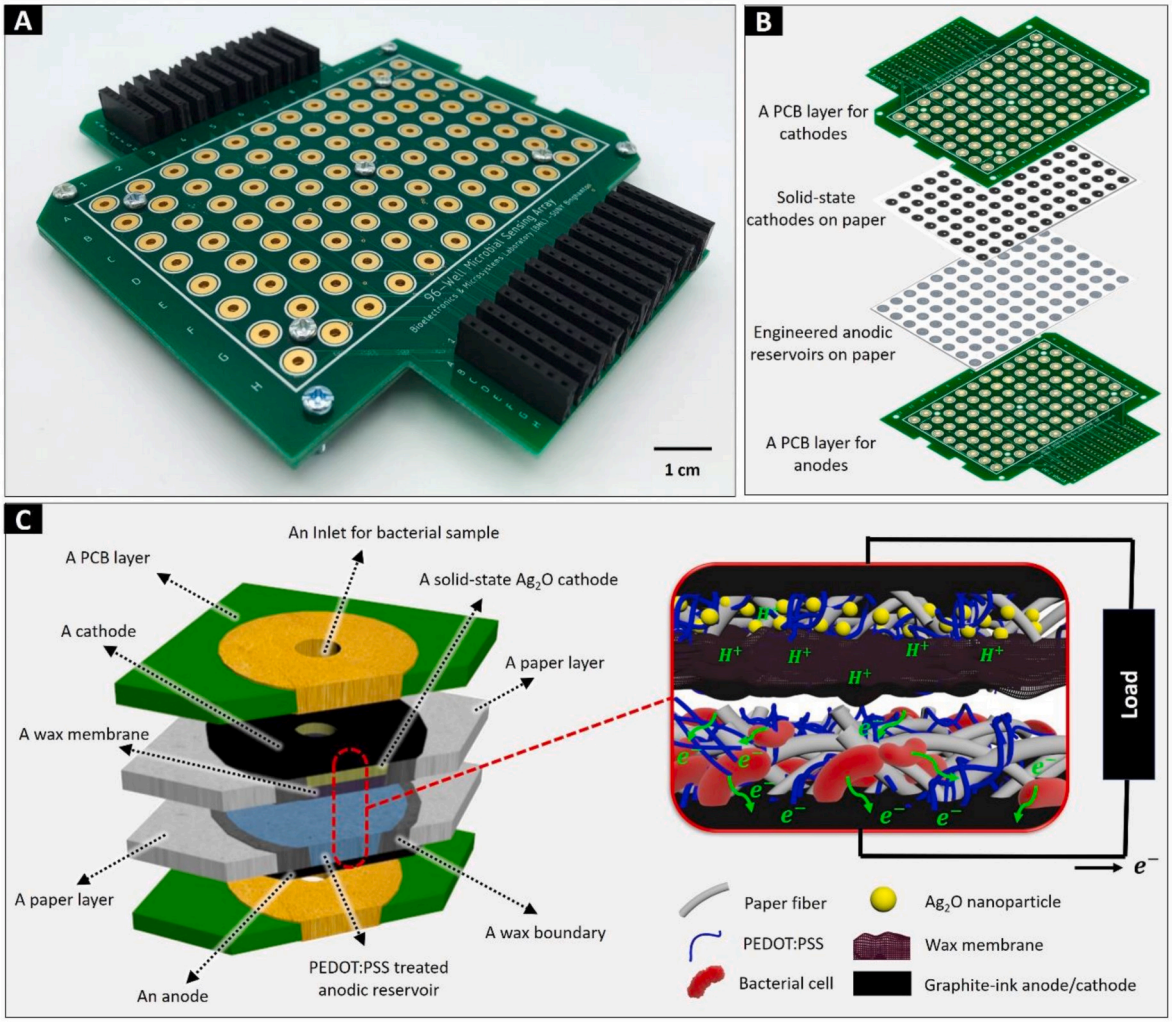

Fig. 2. (A) A photo-image of the 96-well sensing array and (B) a schematic diagram of its individual layers. The paper-based MFC array is sandwiched between top and bottom PCB layers for electrical contact and measurement. (C) Schematic diagram of an individual sensing unit. Bacterial cells introduced through an inlet oxidized the organic matter in the engineered reservoir, completing respiration by transferring electrons to the anode. The electrons move to the cathode through an external load. The protons produced during the microbial metabolism travel through the wax membranes and reach the cathode. By measuring the voltage drop at the load, the microbial EET can be monitored.

depth of the wax during the heating operation. A solid-state Ag_2O cathode was constructed on a paper substrate with an additional graphite electrode for providing structural support and functioning as a current collector (Gao and Choi, 2018). Compared with conventional MFCs that use oxygen or liquid chemicals as the catholyte, using Ag_2O can greatly improve high-power performance as it reduces cathodic over-potential and the variations between the sensing units. The performance improves because there are only two-phase cathodic reactions of Ag_2O and water, thus eliminating low reactant collision probability or low aqueous oxygen solubility. A wax layer was formed under the cathode and was used as a proton exchange membrane (PEM) (Gao and Choi, 2018). The wax provided the hydrophobic property of the paper, separating the anodic compartment from the cathode and allowing protons to pass through efficiently. Each anodic reservoir had a 5 mm diameter and a sub-microliter volume (6.67 μL). A water-dispersed conducting polymer mixture poly(3,4-ethylenedioxythiophene): polystyrene sulfonate (PEDOT:PSS) with dimethyl sulfoxide (DMSO) was introduced into the reservoirs to promote conductivity (Hamedi et al., 2016; Mohammadifar and Choi, 2017). The biocompatible nature of PEDOT:PSS improved bacterial adhesion and subsequent biofilm

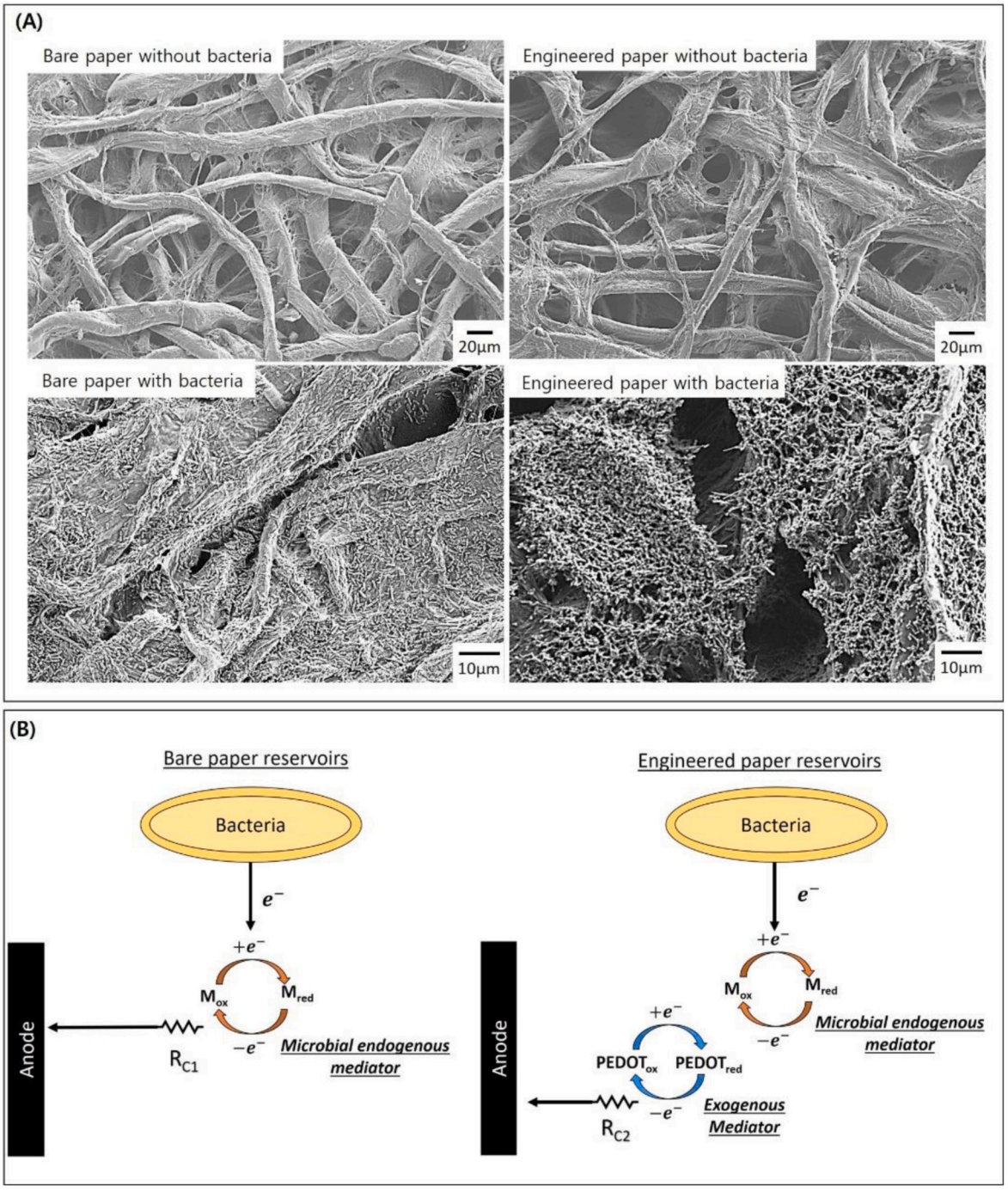

Fig. 3. (A) SEM images of bare and PEDOT:PSS-engineered papers with or without bacterial cells. There is no significant difference in the overall morphology of the paper even after PEDOT:PSS treatment. However, the engineered paper formed a much more densely packed biofilm than the bare one. (B) Schematic diagrams of extracellular electron transfers in bare and engineered paper reservoirs. The use of the redox polymer as a mediator facilitates electron transfer and improve electrical performance of the MFC.

formation (Gao et al., 2019). 3-glycidoxypropy-trimethoxysilane (3-GLYMO) was also introduced into the reservoirs to improve their hydrophilicity for wicking liquid samples via capillary force (Mohammadifar et al., 2018). Fig. 3A shows that this paper engineering did not considerably increase the thickness of the paper fibers, indicating that all the paper fibers were tightly and conformally coated by this mixture without blocking the paper pores, allowing a large surface area for the attachment of the bacteria and their efficient metabolism throughout the porous substratum. Conductive 3-D paper fibers effectively harvest the electrons transferred "directly" from the bacteria attached to the fibers. Furthermore, the redox polymer, PEDOT:PSS, "indirectly" mediate bacterial EET, enhancing the rate of electron transfer and thus electricity generation (Fig. 3B) (Gao et al., 2019; Hamedi et al., 2016). Therefore, our device engineered with the exogenous PEDOT:PSS mediator could provide the rapid and sensitive power assessment of microorganisms even from a sub-microliter sample volume (Fig. 3B). Electrochemical impedance spectroscopy (EIS) measurements evaluated EET efficiency of *P. aeruginosa* on the bare and engineered paper reservoirs (Fig. S2). The EIS results showed a well-defined semicircle followed by a straight line for each reservoir (Gao and Choi, 2018). The intercept of the semicircle with the real impedance axis represented the total anodic resistance (R_{anode}) including the solution resistance (R_S) and the charge transfer resistance (R_C) at the electrode and electrolyte interface. The anodic resistance of the bare paper was estimated to be ~3.8 KΩ, almost 2.5-fold higher than the engineered paper (~1.5 KΩ). The reduced resistance and improved EET efficiency increased the current and power performance of the MFC, thus ultimately resulting in high sensitivity of the screening for bacterial electrogenicity (Fig. S3).

2.2. Selected hypothesis-driven genes in P. aeruginosa that could influence electrogenesis

The first innovative aspect of this study was to use selected isogenic mutants of *P. aeruginosa* as model exoelectrogens to form the customized synthetic microbial community. These mutants were selected based on the hypothesis that significant differences in power density will likely be encountered in some of the mutant strains. Accordingly, we next comprehensively explored the exoelectrogenic capability of wild-type *P. aeruginosa* PAO1 and 95 different isogenic mutants. *P. aeruginosa* is known as a weak exoelectrogen that uses either self-generated, soluble electron mediators or type IV pilus (surface appendages, non-mediator) for their "indirect" EET (Shreeram et al., 2018). We could validate the utility of our novel sensing array by displaying highly comparable performance characteristics and identifying which of the genes in *P. aeruginosa* trigger higher current/power density. *P. aeruginosa* possesses genes for aerobic and anaerobic respiration as well as arginine and pyruvate fermentation (Mohammadifar and Choi, 2017; Shreeram et al., 2018; Liu et al., 2019). The physiological characteristics of the microorganism are well established, in particular, its electron transport system and ability to grow anaerobically, so the microorganism can be engineered for optimal generation of electrical power. For the past several years, many researchers have worked on MFCs with genetically-engineered *P. aeruginosa* using the hypothesis that mutations could alter their electrogenic properties (Shreeram et al., 2018; Liu et al., 2019; Qiao et al., 2017; Yong et al., 2011; Gao et al., 2017). However, no other group has yet to propose or provide a high-throughput parallel analysis of bacterial electrogenicity of nearly 100 genetically-engineered *P. aeruginosa* mutants. The 95 genes that embody hypothesis-driven mutants are listed in Table 1. Those genes were generated using either classical allelic exchange techniques with sucrose counter-selection or transposon mutagenesis (Table S1). Each bacterial strain was tested five times to assess repeatability and reproducibility. A Luria-Broth (LB) medium without bacteria was used as the negative controls while the strong exoelectrogen, *Shewanella oneidensis* MR1, was also tested to study how strategic genetic modifications affect the electrochemical activity of *P. aeruginosa* strains. Both direct EET through physical contacts and indirect EET through endogenous mediators have been identified as main EET mechanism in *S. oneidensis* MR1.

2.3. Automated sample loading and rapid electrical measurement

All bacterial samples were cultivated in an LB medium at 35 °C until the optical density at 600 nm (UV 6300 PC UV-VIS, VWR) reached 2.5 ± 0.2, corresponding to approximately 5.1×10^8 CFU/mL. The cells were harvested by centrifugation at 4000 rpm for 4 min to remove biomass and re-suspended in a 1:1 mixture of culture supernatant and fresh LB medium. An OD_{600} of 2.5 was sufficient to saturate the paper reservoir and optimize MFC performance. Fig. S4 demonstrates that the maximum power density occurred and very densely packed bacteria were observed when an OD_{600} was greater than 2.5. Each bacterial suspension (~5 μL each) was precisely introduced into each sensing unit of the array by using an automated 96-channel pipettor Multimek 96 (Beckman) (Fig. 4A). Our 96-well sensing array demonstrated its compatibility with the standard 96-well micropipettor (Fig. S5). A precise and automatic pipettor provided easy and rapid filling of the array reservoirs. Before characterizing bacterial EETs from the array, we first tested the reproducibility and reliability of the array by measuring the open circuit voltage (OCV) variation from individual MFC units. The OCVs of the 96 MFCs on the array generated 2.8% variation with *P. aeruginosa*. This low percent deviation is mainly because of the miniaturized anodic reservoirs (~5 μL) and reliable/efficient batch-manufacturing operations. After the sample introduction for the characterization of bacterial electrogenicity of the 96 bacterial suspensions, we waited 30 min until the OCV of the unit was stabilized (data not shown). Our paper-based device required only a very short start-up time relative to conventional MFCs (~several days to weeks) for bacterial accumulation and acclimation (Gao and Choi, 2018). The polarization test modules automatically connect varying load resistors to the MFC array (Fig. 4B and Figs. S6–S9). Load resistors were electrically isolated from the controller circuit by solenoid operated relays to eliminate electrical interference. Three data acquisition units (DI-720-EN, DATAQ Instruments, Ohio) were daisy-chained and connected to a computer for synchronous

Table 1
Selected hypothesis-driven mutants of P. aeruginosa

	A	B	C	D	E	F	G	H
1	PAO1	bfrA	galU	lasI	oprF	pilT lasI	rhlI	tonB1
2	abc	ccmC	glpR	lasR	oprH	pilT nirS	rhlI sodA	trxB1
3	acnC	cheB	gor	lasI rhlI	oxyR	pilU	rhlR	uspK
4	ahpA	crc	grx	lasR rhlR	pelA	pmbA	rmd	wapR
5	ahpB	cyoA	hemO	moaA1	PA0612	pilY1	rmlC	wbpL
6	ahpC	dksA	hmgA	motAB	phzM	pmpR	rplY	wbpM
7	algR	dps	hmp	motCD	phzS	prlC	rpoN	PA0079
8	algT(U)	fdnG	hpd	mvfR	pilA	psl pel	rpoS	PA0962
9	arsB	fhp	katA	nirS	pilH	ptxR	snr-1	PA1561
10	atoB	fliC	katB	nirS katA	pilQ	radC	sodA	PA1608
11	azu	fliC pilT	katC	norCB	pilT	recG	sodB	PA1930
12	bdlA	fliD	kauB	ohr	pilT bdlA	relA	tig	PA3236

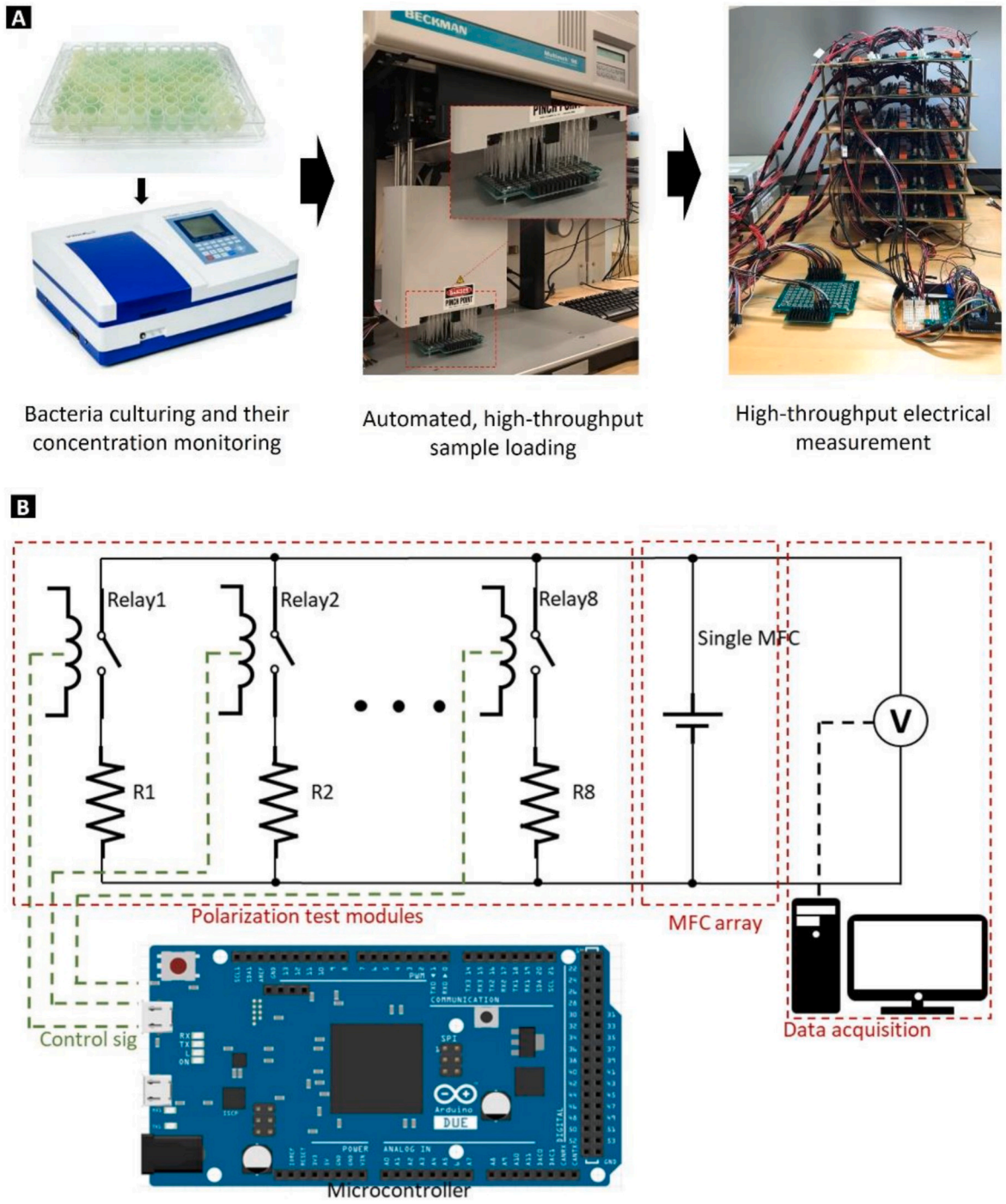

Fig. 4. (A) Test procedure. The cultivated bacterial samples are introduced into each sensing unit of the MFC array by using an automated 96-channel pipettor Multimek 96. (B) Block diagram of electrical measurement set-up for the polarization test. The polarization test modules simultaneously and autonomously measure the electrical outputs from spatially distinct 96 MF units.

voltage measurement. Open circuit voltages (OCVs) were measured while all relays were in the open position. During the polarization test, the output voltages of the MFC units in the array were recorded by data acquisition. Output power and current were calculated by using measured voltages and the corresponding resistance according to Ohm's Law.

2.4. Characterization of microbial EET

The microbial EET can be characterized by three essential parameters; open circuit voltage (OCV), power and current density. These characteristics are usually obtained from polarization and power curves (Logan et al., 2006). The OCV is the potential difference between anode and cathode under open circuit conditions, which is normally lower than the overall device electromotive force because of the overpotentials of the electrodes (Logan et al., 2006; Gildemyn et al., 2017). The overall device output voltage (E_{Device}) is determined by the OCV, the generated current (I) and the internal resistance (R_{int}) of the device, described by (Eqn. (1)):

$$E_{Device} = OCV - I \cdot R_{int} \quad (1)$$

The overall electrogenic performance of microorganisms is evaluated by power output, calculated as

$$P = I \cdot E_{Device} = \frac{E^2_{Decive}}{R_{ext}} \quad (2)$$

where R_{ext} is a fixed external resistor (Eqn. (2)). The power output can be normalized to the projected anode surface area. After the units attained a stable OCV, the overall polarization curves were collected by measuring the voltage across a given external resistance (OCV, 1 MΩ, 500 KΩ, 248 KΩ, 68 KΩ, 45 KΩ, 22 KΩ, 10 KΩ, 5 KΩ, 3.3 KΩ, 2.2 KΩ, 1 KΩ, 0.5 KΩ, 0.33 KΩ and 0.22 KΩ) every 12 s. The power curve is calculated from the polarization curve as a function of current. Therefore, the polarization and power curves are the most important characteristic values that represent an overall measurement of microbial electrogenicity, providing OCV, power, and current as well as electrode overpotential and internal resistance. The polarization and power curves were rapidly obtained by the high-throughput parallel analysis on the array including *P. aeruginosa* and their 95 isogenic mutants (Fig. S10).

Fig. 5. (A) OCV, (B) maximum power density, and (C) current density at the maximum power are obtained from the polarization and power curves by the high-throughput parallel analysis on the array. The power and current outputs are normalized to the projected anode surface area.

Additionally, those curves were obtained from *S. oneidensis* MR1 and media without bacteria as the controls. Fig. 5 summarizes the OCV, the maximum power density, and the current density at the maximum power for all bacterial samples including controls. The OCVs range from 0.32 to 0.54 V while the LB medium has very low OCV (0.12 V). The OCV values generated from our MFC array are much higher than those of typical microscale MFCs (~0.3 V), indicating that our device considerably improved sensitivity and power assessment. Of 95 *P. aeruginosa* mutants, four produced higher OCV values than the wild-type control strain, PAO1*; fliC, pmpR, algT(U)* and *acnC*. The *fliC* mutant lacks flagellin that prohibits swimming motility (Brimer and Montie, 1998), while still improving bacterial adhesion to the anode via type IV pili and reducing the anode overpotential. In contrast, the *pmpR* mutant improves swarming motility but increased the OCV (Shen et al., 2014). The *pmpR* gene encodes a YebC-like negative regulator of quorum sensing. As such, it is not surprising that Liang et al. showed that a *pmpR* mutant generated higher levels of the quorum sensing-controlled, electrogenic mediator, pyocyanin (Liang et al., 2008). Our *pmpR* mutant consistently overproduced the mediator pyocyanin in broth and agar media (Fig. 6A–C) Bacteria that overproduce pyocyanin as well as its red redox-active precursor, pyorubrin (aeruginosin A), demonstrated increase power generation relative to wild-type bacteria (Liang et al., 2008). As shown in Fig. 5, the power density and the current density at the maximum power of the *pmpR* mutant were also higher than the wild-type control. The *algT(U)* and *acnC* mutants inactivate the production of the virulence factors, alginate (Martin et al., 1993) and aconitase (Somerville et al., 1999), respectively, but further studies are required to determine how inactivation of such genes increase the OCV values. Furthermore, our results yielded power density measurements of 95 bacterial mutants of *P. aeruginosa* and its wild-type control strain. The highest power density and current density at the maximum power were observed from the *hmgA* mutant, followed by *pmpR* and *pel psl*. Their power and current generations were much higher than even strong electrogen, *S. oneidensis* MR1. The *hmgA* gene encodes homogentisate-1, 2-dioxygenase that is involved in the tyrosine and phenylalanine degradation pathways (Fig. 6D–F) (Yoon et al., 2007). Mutants lacking *hmgA* accumulate homogentisate (HGA). Once secreted from the cell, HGA auto-oxidizes, and self-polymerizes to form the brown to black, negatively charged pyomelanin (Fig. 6D & E). The addition of pyomelanin to wild-type bacteria using our MFC platform increased the power

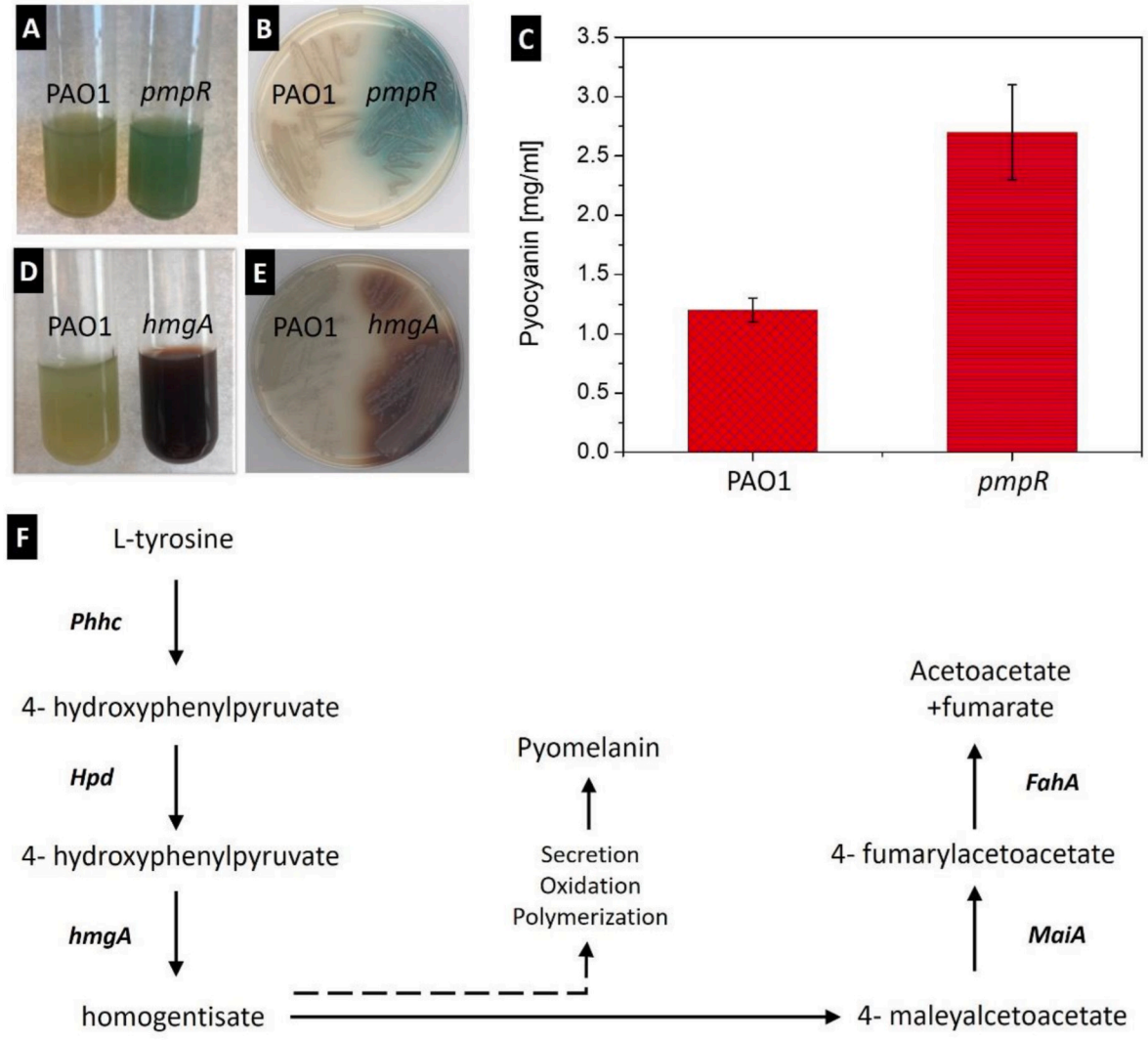

Fig. 6. (A) Wild-type and *pmpR* mutant bacteria were grown in LB broth for 24 h. Note the enhanced blue color due to pyocyanin overproduction in the *pmpR* mutant. (B) Wild-type and *pmpR* mutant bacteria were streaked on aerobic LB agar medium and incubated for 24 h. Again, note the enhanced blue color secreted into the agar. (C) Quantification of pyocyanin in broth cultures (n = 3) of wild-type vs. the *pmpR* mutant. (D) Wild-type and *hmgA* mutant bacteria were grown aerobically for 24 h. Note the dark brown/black pyomelanin produced during autoxidation. (E) Wild-type and *hmgA* mutant bacteria were streaked on aerobic LB agar and grown for 48 h prior to photography. Note the brownish pyomelanin secreted into the agar medium. (F) The tyrosine-phenylalanine degradation pathway leading to the production of pyomelanin. (For interpretation of the references to color in this figure legend, the reader is referred to the Web version of this article.)

density (Turick et al., 2002). Oxidative stress from peroxide is decreased in *P. aeruginosa* as a result of pyomelanin production, ultimately increasing their power generation in the MFC. In contrast, the *pel* and *psl* genes are responsible for the production of polysaccharides that contribute to the three-dimensional structure of biofilms (Colvin et al., 2012). Polysaccharide in the biofilm matrix allows for structural integrity and resistance to environmental factors, antibiotics, and biocides. They also can impede nutrient flow to organisms within the biofilms which would decrease overall power density in an MFC. We believe that reduced polysaccharide in the *pel psl* mutant allows for enhanced electrogenic properties. Further studies are required to fully understand the effects of these genetic modifications on electrogenic capabilities. However, this work will create a compact screening system that is individually addressable for identification and characterization of electrochemically active microbes, paving the way to a new era of electromicrobiology.

3. Conclusion

In this work, we created an inexpensive, scalable, time-saving, high-performance and user-friendly platform that facilitated studies of fundamental bacterial electrogenicity. 96 MFC units could be batch-fabricated on paper by spraying or screen-printing materials and forming hydrophilic microfluidic regions with asymmetrical hydrophobic wax patterns. This MFC array system was carefully designed and assembled on paper using numerous strategies and materials, especially focusing on the development of the fluidic reservoirs, the fluidic and electric interconnections, and the electrical interfaces on a large array format. Spatially distinct 96 wells of the MFC array provided high-throughput measurements and highly comparable performance characteristics for screening 95 isogenic mutants of *P. aeruginosa*. Better electrical performance produced by the *hmgA*, *pmpR* and *pel psl* mutants compared with the wild-type was quite interesting because it indicated how strategic genetic modifications affect the electrochemical activity of bacteria. Our innovative MFC array could drive the development of novel paradigms for genetic networks that help develop mutations or over-expression constructs and identify which genes in *P. aeruginosa* trigger higher electrical performance.

4. Experimental sections

4.1. Materials

Whatman™ Grade 3 MM Chromatography Paper and Graphite ink were provided from Fisher Scientific Company, LLC. Ag_2O (11,407–14) was purchased from Alfa Aesar. Poly(3,4-ethylenedioxythiophene): polystyrene sulfonate (PEDOT:PSS) (Clevios PH1000) was obtained from Heraeus. Dimethyl sulfoxide (DMSO) and 3-glycidoxypropy-trimethoxysilane (GLYMO) were purchased from Sigma-Aldrich.

4.2. Preparation of paper-based sensing array

A 96-well sensing array was designed on two sheets of paper layers; therein, 96 individual MFC devices were batch-fabricated. The 96 hydrophilic reservoirs were first defined with hydrophobic wax boundaries on the anodic paper layer simply by using a Xerox ColorQube wax printer and letting the wax melt into the paper by heating the paper in an oven at 150° for 30 s (Fig. S1). The mixture of 1 wt% of PEDOT:PSS and 5 wt% of DMSO was added with a multichannel pipette into the reservoirs defined by the wax. A 2 wt% of GLYMO solution was subsequently added to the engineered reservoirs to increase the capillary force of the paper (Mohammadifar et al., 2018). The solutions were allowed to dry through evaporation at room temperature. For the cathodic paper layer, the wax defined the cathodic reservoir for the introduction of the mixture of Ag_2O in PEDOT:PSS solution. The wax printed on the bottom of the cathodic layer was used as the proton exchange membrane (PEM). Then, graphite ink was screen-printed on top of the anodic and cathodic layers, respectively, as the current collector. Finally, the layers were put together to form 96 MFC units (Fig. S1).

4.3. Printed circuit board (PCB) design and preparation

Using the free version of PCB design software (Eagle), we designed the circuit diagram, the route of the wires and layout of the electronic components on a two-layer printed circuit board (PCB) (Fig. 4B, Figs. S5–S9). The design of the PCB was verified by design rule check and fabricated through a commercial custom PCB service (PCBWay, Shenzhen, China). For the 96-well sensing array, two PCBs were designed for anodic and cathodic electrical contact, respectively, with engineered paper-based reservoir and solid-state paper cathode (Fig. 2B). For the electrical measurement interface (Fig. 4B), all circuit components shown in Fig. S6 were obtained from Digi-Key Electronics. The polarization test modules (PTM) were designed to automatically connect load resistors to the MFC array. As the interface between the microcontroller (Arduino DUE) and the PTM, signal-latch ICs (CD74HC75E) were used to reduce current drawn from the microcontroller (Fig. S6). Double pole double throw (DPDT) relays (EC2-5NU, NEXEM, Japan) were used in the PTM to minimize the circuit component number (Fig. S7). Thus, each module supported 2 MFC units (Fig. S8). Pull-down resistors (470 KΩ) were connected to the control signal wires from the microcontroller to PTM (Fig. S9).

4.4. Bacterial inoculum

P. aeruginosa PAO1 mutants were generated using classical allelic replacement techniques with sucrose counter-selection as described by Hoang et al. or by transposon (Tn) mutagenesis using a mini transposon vector, pBT20 (Kulasekara et al., 2015). All bacterial strains were grown in LB media (1 w/v% tryptone, 0.5 w/v% yeast extract and 0.5 w/v% NaCl) with the cell titers controlled by monitoring the optical density at 600 nm. The detailed information of 95 genetically engineered *P. aeruginosa* is described in Table 1S. *Pseudomonas aeruginosa* isogenic mutants were constructed using three different techniques. Briefly, insertional mutagenesis was performed using an 850 bp GMR cassette from pUCGM (Schweizer, 1993) and the gene replacement vector pEX100T-KS (Schweizer and Hoang, 1995). Unmarked deletion mutants were constructed by the method of Choi and Schweizer (2005) by overlap extension PCR, subsequent cloning into the Gateway vector, pDONR221, and recombined into the chromosome using the gene replacement vector, pEX18ApGW. Transposon mutagenesis was performed using the mariner transposon vector, pBT20, that was conjugally transferred into strain PAO1 by biparental mating using *E. coli* S17-1 λ pir (Kulasekara et al., 2015).

4.5. Bacterial fixation and SEM imaging

The SEM samples were treated with 4% glutaraldehyde solution (Sigma-Aldrich) overnight at 4 °C and rinsed three times with 0.1 M phosphate buffer saline (PBS) (Van Neerven et al., 1990). The samples were then dehydrated by 5-min serial transfers through 50, 70, 80, 90, 95, and 100% ethanol. The samples were placed in hexamethyldisilazane (HMDS) right after for 10 min and then placed in desiccator to air dry overnight. Fixed samples were examined using a FESEM (Field Emission SEM) (Supra 55 VP, Zeiss).

Declaration of competing interest

The authors declare that they have no known competing financial interests or personal relationships that could have appeared to influence the work reported in this paper.

CRediT authorship contribution statement

Mehdi Tahernia: Investigation, Methodology, Data curation, Writing - original draft. **Maedeh Mohammadifar:** Investigation, Formal analysis, Writing - original draft. **Yang Gao:** Investigation, Writing - original draft. **Warunya Panmanee:** Investigation. **Daniel J. Hassett:** Investigation, Formal analysis, Funding acquisition, Writing - review & editing. **Seokheun Choi:** Conceptualization, Supervision, Project administration, Funding acquisition, Writing - review & editing.

Acknowledgments

This work was supported by the National Science Foundation (ECCS #1703394 & #1920979), Office of Naval Research (#N00014-81-1-2422), and the SUNY Binghamton Research Foundation (SE-TAE) to S.C. Other support was a sub-contract from the National Science Foundation (CBET #1605482) to D.J.H.

Appendix A. Supplementary data

Supplementary data to this article can be found online at https://doi.org/10.1016/j.bios.2020.112259.

References

Alfonta, L., 2010. Genetically engineered microbial fuel cells. Electroanalysis 22, 822–831.
Biffinger, J., Ribbens, M., Ringeisen, B., Pietron, J., Finkel, S., Nealson, K., 2009. Characterization of electrochemically active bacteria utilizing a high-throughput voltage-based screening assay. Biotechnol. Bioeng. 102, 436–444.
Brimer, C.D., Montie, T.C., 1998. Cloning and comparison of fliC genes and identification of glycosylation in the flagellin of *Pseudomonas aeruginosa* a-type strains. J. Bacteriol. 180, 3209–3217.
Cao, X., Huang, X., Zhang, X., Liang, P., Fan, M., 2009. A mini-microbial fuel cell for voltage testing of exoelectrogenic bacteria. Front. Environ. Sci. Eng. China 3, 307–312.
Chabert, N., Ali, O.A., Achouak, W., 2015. All ecosystems potentially host electrogenic bacteria. Bioelectrochemistry 106, 88–96.
Choi, K.H., Schweizer, H.P., 2005. An improved method for rapid generation of unmarked Pseudomonas aeruginosa deletion mutants. BMC Microbiol. 5, 30.
Colvin, K.M., Irie, Y., Tart, C.S., Urbano, R., Whitney, J.C., Ryder, C., Howell, P.L., Wozniak, D.J., Parsek, M.R., 2012. The *Pel* and *Psl* polysaccharides provide *Pseudomonas aeruginosa* structural redundancy within the biofilm matrix. Environ. Microbiol. 14, 1913–1928.
E Doyle, L., Marsili, E., 2018. Weak electricigens: a new avenue for bioelectrochemical research. Bioresour. Technol. 258, 354–364.
Gao, Y., Choi, S., 2018. Merging electric bacteria with paper. Advanced Materials Technologies 3, 1800118.
Gao, Y., Hassett, D., Choi, S., 2017. Rapid characterization of bacterial electrogenicity using a single-sheet paper-based electrofluidic array. Frontiers in Bioengineering and Biotechnology 5, 44.
Gao, Y., Mohammadifar, M., Choi, S., 2019. From microbial fuel cells to Biobatteries: moving toward on-demand micro-power generation for Small-scale Single-Use Applications. Advanced Materials Technologies. https://doi.org/10.1002/admt.201900079.
Gildemyn, S., Rozendal, R.A., Rabaey, K., 2017. A gibbs free energy-based assessment of microbial electrocatalysis. Trends Biotechnol. 35, 393–406.
Hamedi, M.M., Ainla, A., Guder, F., Christodouleas, D.C., Fernandez-Abedul, M., Whitesides, G.M., 2016. Integrating electronics and microfluidics on paper. Adv. Mater. 28, 5054–5063.
Hou, H., Li, L., Cho, Y., de Figueiredo, P., Han, A., 2009. Microfabcricated microbial fuel cell arrays reveal electrochemically active microbes. PloS One 4, e6570.
Hou, H., Li, L., Ceylan, C.U., Haynes, A., Cope, J., Wilkinson, H.H., Erbay, C., de Figueiredo, P., Han, A., 2012. A microfluidic microbial fuel cell array that supports long-term multiplexed analyses of electricigens. Lab Chip 12, 4151–4159.
Koch, C., Harnisch, F., 2016a. What is the essence of microbial electroactivity? Front. Microbiol. 7, 1890.
Koch, C., Harnisch, F., 2016b. Is there a specific ecological niche for electroactive microorganisms? ChemElectroChem 3, 1282–1295.
Kouzuma, A., Kato, S., Watanabe, K., 2015. Microbial interspecies interactions: recent findings in syntrophic consortia. Front. Microbiol. 6, 477.
Kulasekara, H.D., Ventre, I., Kulasekara, B.R., Lazdunski, A., Filoux, A., Lory, S., 2015. A novel two-component system controls the expression of *Pseudomonas aeruginosa* fimbrial *cup* genes. Mol. Microbiol. 55, 368–380.
Kumara, A., Hsu, H.H., Kavanagh, P., Barrière, F., Lens, P.N.L., Lapinsonnière, Laure, Lienhard V, J., Schröderg, U., Jiang, X., Leech, D., 2017. The ins and outs of microbial-electrode electron transfer reactions. Nature Rev. Chem. 1, 0024.
Liang, H., Li, L., Dong, Z., Surette, M.G., Duan, K., 2008. The YebC family protein PA0964 negatively regulates the *Pseudomonas aeruginosa* quinolone signal system and pyocyanin production. J. Bacteriol. 190, 6217–6227.
Light, S.H., Su, L., Rivera-Lugo, R., Cornejo, J.A., Louie, A., Iavarone, A.T., Ajo-Franklin, C.M., Portnoy, D.A., 2018. A flavin-based extracellular electron transfer mechanism in diverse Gram-positive bacteria. Nature 562, 140–144.
Liu, X., Wang, S., Xu, A., Zhang, Li, Liu, H., Ma, L.Z., 2019. Biological synthesis of high-conductive pili in aerobic bacterium *Pseudomonas aeruginosa*. Appl. Microbiol. Biotechnol. 103, 1535–1544.
Logan, B.E., Hamelers, B., Rozendal, R., Schröder, U., Keller, J., Freguia, S., Aelterman, P., Verstraete, W., Rabaey, K., 2006. Microbial fuel cells: methodology and technology. Environmental Science & Technology 40, 5181–5192.
Logan, B.E., Rossi, R., Ragab, A., Saikaly, P.E., 2019. Electroactive microorganisms in bioelectrochemical systems. Nat. Rev. Microbiol. 17, 307–319.
Lovley, D.R., 2012. Electromicrobiology. Annu. Rev. Microbiol. 66, 391–409.
Lovley, D.R., 2017. Syntrophy goes electric: direct interspecies electron transfer. Annu. Rev. Microbiol. 71, 643–664.
Martin, D.W., Holloway, B.W., Deretic, V., 1993. Characterization of a locus determining the mucoid status of *Pseudomonas aeruginosa: AlgU* shows sequence similarities with a *Bacillus* sigma factor. J. Bacteriol. 175, 1153–1164.
Mohammadifar, M., Choi, S., 2017. A papertronics, on-demand and disposable biobattery: saliva-activated electricity generation from lyophilized exoelectrogens pre-inoculated on paper. Advanced Materials Technologies 2, 1700127.
Mohammadifar, M., Zhang, J., Yazgan, I., Sadik, O., Choi, S., 2018. Power-on-paper: origami-inspired fabrication of 3-D microbial fuel cells. Renew. Energy 118, 695–700.
Mukherjee, S., Su, S., Panmanee, W., Irvin, R.T., Hassett, D.J., Choi, S., 2013. A microliter-scale microbial fuel cell array for bacterial electrogenic screening. Sensor Actuator Phys. 201, 532–537.
Park, J., Kang, H., Park, K., Park, H., 2018. Direct interspecies electron transfer via conductive materials: a perspective for anaerobic digestion applications. Bioresour. Technol. 254, 300–311.
Qian, F., Baum, M., Gu, Qian, Morse, D.E., 2009. A 1.5 μL microbial fuel cell for on-chip bioelectricity generation. Lab Chip 9, 3076–3081.
Qiao, Y., Qiao, Y., Zou, L., Wu, X., Liu, J., 2017. Biofilm promoted current generation of *Pseudomonas aeruginosa* microbial fuel cell via improving the interfacial redox reaction of phenazines. Bioelectrochemistry 117, 34–39.
Schröder, U., 2011. Discover the possibilities: microbial bioelectrochemical systems and the revival of a 100-year-old discovery. J. Solid State Electrochem. 15, 1481–1486.
Schweizer, H.P., 1993. Small broad-host-range gentamicin resistance gene cassettes for site-specific insertion and deletion mutagenesis. Biotechniques 15, 831–833.
Schweizer, H.P., Hoang, T.T., 1995. An improved system for gene replacement and xylE fusion analysis in Pseudomonas aeruginosa. Gene 158, 15–22.
Shen, H., Yong, X., Chen, Y., Liao, Z., Si, R., Zhou, J., Wang, S., Yong, Y., OuYang, P., Zheng, T., 2014. Enhanced bioelectricity generation by improving pyocyanin production and membrane permeability through sophorolipid addition in *Pseudomonas aeruginosa*-inoculated microbial fuel cells. Bioresour. Technol. 167, 490–494.
Shreeram, D.D., Panmanee, W., McDaniel, C.T., Daniel, S., Schaefer, D.W., Hassett, D.J., 2018. Effect of impaired twitching motility and biofilm dispersion on performance of *Pseudomonas aeruginosa*-powered microbial fuel cells. J. Ind. Microbiol. Biotechnol. 45, 103–109.
Slate, A.J., Whitehead, K.A., Brownson, D.A.C., Banks, C.E., 2019. Microbial fuel cells: an overview of current technology. Renew. Sustain. Energy Rev. 101, 60–81.
Somerville, G., Mikoryak, C.A., Reitzer, L., 1999. Physiological characterization of *Pseudomonas aeruginosa* during exotoxin A synthesis: glutamate, iron limitation, and aconitase activity. J. Bacteriol. 181, 1072–1078.
Tahernia, M., Mohammadifar, M., Hassett, D.J., Choi, S., 2019. A fully disposable 64-well papertronic sensing array for screening electroactive microorganisms. Nanomater. Energy 65, 104026.
TerAvest, M.A., Ajo-Franklin, C.M., 2016. Transforming exoelectrogens for biotechnology using synthetic biology. Biotechnol. Bioeng. 113, 687–697.
Turick, C.E., Tisa, L.S., caccavo Jr., F., 2002. Melanin production and use as a soluble electron shuttle for Fe(III) oxide reduction and as a terminal electron acceptor by *Shewanella algae* BrY. Appl. Environ. Microbiol. 68, 2436–2444.
Van Neerven, A.R., Wijffels, R., Zehnder, A.J., 1990. Scanning electron microscopy of immobilized bacteria in gel beads: a comparative study of fixation methods. J. Microbiol. Methods 11, 157–168.
Wang, Q., Ill, A.D.J., Gralnick, J.A., Lin, L., Buie, C.R., 2019. Microfluidic dielectrophoresis illuminates the relationship between microbial cell envelope polarizability and electrochemical activity. Science Advances 5, eaat5664.
Yates, M.D., Eddie, B.J., Kotloski, N.J., Lebedev, N., Malanoski, A.P., Lin, B., Strycharz-Glavena, S.M., Tender, L.M., 2016. Toward understanding long-distance extracellular electron transport in an electroautotrophic microbial community. Energy Environ. Sci. 9, 3544–3558.
Yong, Y., Yu, Y., Li, C., Zhong, J., Song, H., 2011. Bioelectricity enhancement via overexpression of quorum sensing system in *Pseudomonas aeruginosa*-inoculated microbial fuel cells. Biosens. Bioelectron. 30, 87–92.
Yoon, S.S., Karabulut, A.C., Lipscomb, J.D., Hennigan, R.F., Lymar, S.V., Groce, S.L., Herr, A.B., Howell, M.L., Kiley, P.J., Schurr, M.J., Gaston, B., Choi, K.H., Schweizer, H.P., Hassett, D.J., 2007. Two-pronged survival strategy for the major cystic fibrosis pathogen, *Pseudomonas aeruginosa*, lacking the capacity to degrade nitric oxide during anaerobic respiration. EMBO J. 26, 3662–3672.
Zhou, S., Wen, J., Chen, J., Lu, Q., 2015. Rapid measurement of microbial extracellular respiration ability using a high-throughput colorimetric assay. Environ. Sci. Technol. Lett. 2, 26–30.